The multi-faceted X-ray activity of a complete sample of low-redshift galaxies

1. Scientific Justification

Radio galaxies are excellent subjects for studies of the physics of active galactic nuclei (AGN)

- because their steep-spectrum, large-scale, emission is not relativistically beamed, and so can be used to define a complete, orientation-independent, sample;
- because VLA and VLBI data for their small-scale central structures give rough orientation constraints for their jets and so their beamed emission; and
- because many lie at $z < 0.1$, so that excellent structural information can be obtained and the source components can be spatially separated.

Under unified schemes, radio galaxies are the likely parent population of quasars and BL Lac objects. If the jet of a high-power (FR II, usually lobe- and hot-spot-dominated) radio galaxy lies close to the line of sight, relativistic boosting will cause the AGN to appear as a quasar. If the jet is in a low-power (FR I, usually kpc jet-dominated) radio galaxy, the result will be a BL Lac object. Studies of nearby radio galaxies then elucidate the physics of components of quasars and BL Lacs which are otherwise hard to study both because of their greater distances, and because of dynamic range problems between their bright cores and the fainter, extended structures.

Fabbiano et al. (1984)'s early work on the X-ray properties of radio galaxies detected 65% of a sample of 40 objects. Although FR-II radio galaxies were found to have higher X-ray luminosities than FR-I radio galaxies, *Einstein*'s IPC did not have the angular resolution to determine which structural or spectral components contribute to that luminosity. Several different explanations for the correlation remained viable until ROSAT, which resolved sources into cores and extended emission. The X-ray and radio core fluxes were then shown to be correlated. This implies that a significant part of the core X-ray emission is associated with a relativistic jet (Worrall & Birkinshaw 1994). However only four X-ray jets were detected with *Einstein* or ROSAT, and so only indirect conclusions could be drawn about the jet physics.

The sub-arcsec angular resolution and high sensitivity of *Chandra* changed the picture dramatically, providing detailed information on the physics of the many components of radio galaxies. *Chandra* has measured the properties of regions near massive black holes, e.g. in the core of M 87 = 3C 274 (Wilson & Yang 2002, di Matteo et al. 2003). *Chandra*'s sub-arcsec imaging of X-ray synchrotron radiation from jets has allowed their populations of relativistic electrons to be inferred, e.g., in 3C 66B (Hardcastle et al. 2001). The interactions between the ambient thermal gas and the relativistic jet plasma cause a variety of bubble structures, e.g., in NGC 1275 = 3C 84 (Fabian et al. 2000, 2003) and M 84 = 3C 272.1 (Finoguenov & Jones 2001). The structure of the atmospheres near jets has been measured through their thermal X-ray emission, and in 3C 31 (Hardcastle et al. 2002a, Laing & Bridle 2002) the jet/gas interactions match a self-consistent jet flow model. Strong shocks at jet terminations lead to bright inverse-Compton emission, e.g., in 3C 330 (Hardcastle et al. 2002b), although synchrotron radiation may be important in some cases, e.g., 3C 390.3 (Harris et al. 1998). Finally, lobe inverse-Compton emission is often present, e.g. in 3C 263 (Hardcastle et al. 2002b), permitting magnetic field measurements.

However *Chandra* has not yet taken full advantage of the possibilities afforded by radio galaxies because no large complete sample has been observed, and because much of the work on high-power sources has been done at high redshift, where the structural information is poorer. It is crucial that low-redshift radio galaxies are studied in detail to determine a reference range of properties for source components in different classes of AGN. Thus the main purpose of the current proposal is to complete *Chandra* observations of the lowest-redshift, best-studied, complete sample of radio galaxies, to allow reliable conclusions to be drawn about individual objects, and hence to provide the foundation for further work on the AGN population as a whole.

Figure 1. Radio luminosity at 178 MHz (isotropic power) plotted against redshift for the $z < 0.1$ 3CRR sample. Triangles, squares, and circles represent the FR I, FR I/II, and FR II sources. Filled symbols show sources proposed for 40 ks *Chandra* observations.

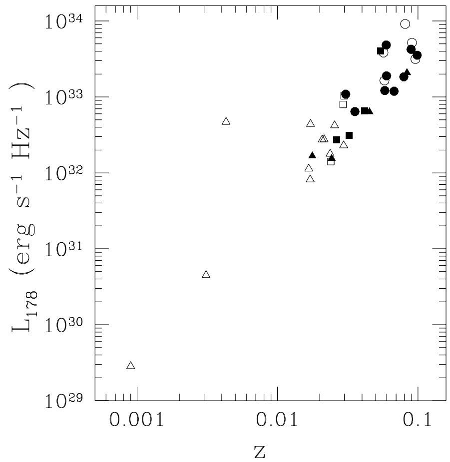

We base our work on the 3CRR sample (Laing et al. 1983), which lies at high declination and galactic latitude, has high-quality radio (VLA and often VLBI), infra-red (ISO, Tansley et al. 2004), optical and UV (usually HST), and some good X-ray data. 3CRR was based on a 178-MHz survey, and provides an almost orientation-independent set of AGN since most 178-MHz flux density comes from extended, unbeamed, emission. 3CRR at low redshift ($z < 0.1$) contains several overlapping subsamples (Table 1), and covers a factor $\sim 10^4$ in radio power (Fig. 1).

- 14 of the sources are FR I and 14 are FR II, with 7 of transitional (FR I/II) type, and one starburst galaxy (3C 231 = M 82).
- 22 sources display only low excitation lines, and 14 have strong lines.
- 9 galaxies are relatively isolated, 10 are in significant groups, and 17 are in clusters of galaxies.

Thus the 3CRR sample to $z = 0.1$ contains enough objects in each of the main AGN classes that differences between them can be investigated. A smaller sample would make class/class comparisons harder, since the subsamples would have too few members. Incomplete X-ray coverage at the current level (Table 1) renders unreliable many statements about the relationship between different X-ray components (e.g., the brightnesses of the X-ray jets and the density of the nearby atmosphere), even where there exist models that predict such relationships.

The redshift range over which these radio galaxies must be studied is dictated by the source powers (Fig. 1). The lowest-redshift ($z < 0.05$) radio galaxies are of low power, and are representative of the low-activity AGN found in the deepest X-ray surveys. Many are famous objects and so have been well observed with *Chandra* (Table 1). The highest-power sources appear only at the highest redshifts, and detailed structural studies of these FR II radio galaxies, which are the dominant radio-emitting population in most high-redshift AGN samples, are possible with *Chandra* out to $z = 0.1$, where the 0.5 arcsec FWHM of the *Chandra* PRF corresponds to linear scales of less than 1 kpc. The full range of radio source morphologies is only covered in 3CRR when the sample extends to $z \sim 0.1$.

Even at the lowest redshifts and powers, a sample of only five AGN (we exclude 3C 231) can be selected before incompleteness becomes apparent, because the lowest-power twin-lobe FR-I (3C 386) has not been observed. The sample of nearby FR II AGN is more seriously incomplete, since it is only $\sim 30\%$ observed (Table 1). In view of the fundamental importance of the 3CRR sample for AGN studies, we believe it is crucial that the sample be completely observed with *Chandra*'s imaging spectroscopy while ACIS's efficiency remains good.

We list a few of the investigations that we intend to undertake with the complete sample.

(1) We will exploit *Chandra*'s spatial resolution to examine the jet-related X-ray structures at the centres of many of these galaxies (e.g., Fig. 3). Our earlier work found offsets between the

radio and X-ray centroids of knots in the jets, and showed that the radio to X-ray spectra of many jets were similar. However, this work was based on the brightest radio jets, and the selection may have biased the sample to the most beamed cases, so that our conclusions on particle acceleration may not be secure.

(2) High spatial resolution is crucial for any investigation of the interaction between the jets and the external medium. It has repeatedly been demonstrated (e.g., in 3C 272.1) that the radio plasma can evacuate regions of thermal gas, but there are examples where the reverse is true. An example is 3C 442A (Fig. 2) where the radio plasma appears to be distorted by a bubble of thermal material. If both types of interaction are common, then the internal and external pressures of the radio galaxies must be relatively well balanced whereas for high-redshift FR II it appears that the lobes are significantly underpressured in relativistic electrons and magnetic fields. This test has important implications for the particle content of the lobes.

(3) In combination with low-z 3CRR data from the GTO *HST* and *Spitzer* programs and in their archives, it will be possible to make sensitive tests of models of jet particle acceleration by constructing SEDs as full as those for 3C 274 (= M 87; Perlman & Wilson 2004).

(4) For most of the FR II radio galaxies the hot spots will fall on the detector. The resulting low redshift hot-spot sample will be compared with the high-redshift sample already in hand. Simple inverse-Compton models do not always explain the X-ray or optical brightnesses of hot spots at high redshift, and *Chandra*'s high linear resolution in the $z < 0.1$ sample will let us search for structural effects that can elucidate this anomaly and test competing models (Georganopoulos & Kazanas 2002; Brunetti et al. 2003).

(5) We will investigate the X-ray properties of radio galaxies near the FR I/FR II boundary to test the idea that gas properties are the controlling parameter in defining the location of this boundary, rather than the optical magnitude of the host galaxy (Owen & Ledlow 1994). We can also test the relationship between the central accretion rate and radio properties of AGN (di Matteo et al. 2003). The paucity of good X-ray observations at $z \sim 0.05$ (Table 1) currently makes both investigations impossible.

We are acutely aware of the legacy aspect of this proposal. It is essential that the best-studied radio sample of active galaxies receives arcsec-resolution X-ray imaging, without which there will remain doubts about selection effects in the interpretation of X-rays from distant active galaxies. The legacy concept also leads us to request eight HST orbits to complete the imaging programme started by the Snapshot Survey (Martel et al. 20000 and references therein). Most of the low-z 3CRR sources have been observed with HST, and the data have provided invaluable information on jet emission, UV light from the AGN, the distribution of stars near the cores, and the dust lanes that overlie the AGN and absorb some of the X-rays (e.g., de Koff et al. 2000, Hardcastle & Worrall 2000, Chiaberge et al. 2002). However, for eight objects incomplete or no HST data are available. To provide a uniform dataset we propose to image these galaxies in the missing bands for a total of one orbit per galaxy. The complete HST dataset for low-z 3CRR objects will be useful for the interpretation of many other datasets including those from *Chandra* and *Spitzer*.

2. Technical Feasibility for the *Chandra* Observations

The low-redshift 3CRR sample has been 53% observed with *Chandra* over the past 5 AOs, but the rate of observation of these sources has declined as a function of AO number. To complete the sample a targetted proposal such as this is necessary. All but one of the sample objects has been observed with ACIS-S, with a median observing time ~ 40 ks. Investigations by the original observers, and in the *Chandra* archive show that 40 ks is sufficient to allow the study of all major features of the radio galaxies, even the most distant (Fig. 3). We therefore adopt 40 ks as the standard observing time for this proposal.

The low-z 3CRR have a wide range of angular sizes, but most of the physical processes lead

Figure 2. The 1.4-GHz radio image of 3C 442A (grey-scale) with ROSAT HRI contours smoothed by a Gaussian with $\sigma = 16$ arcsec. The inset shows the ROSAT HRI data smoothed with $\sigma = 4$ arcsec on an optical image of the nuclei of NGC 7237 (center) and its companion NGC 7236 (to the NW). The central X-ray structure contains a component from the AGN in NGC 7237, but the brighter component seems to represent a dense bubble of hot gas between the central filaments. From Hardcastle & Worrall (1999).

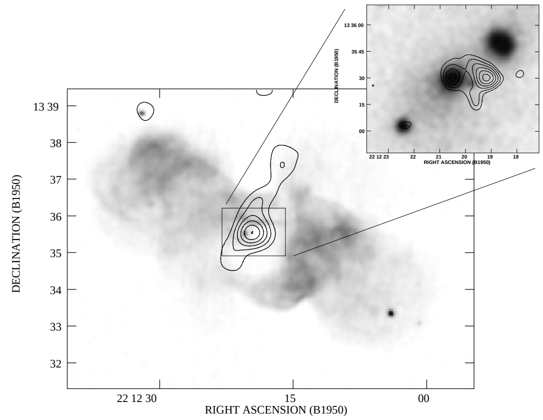

to X-ray structures concentrated in the central 2 arcmin of the fields, where bright jet features and gas/radio plasma interactions will be found. We therefore choose to observe the sources at the standard aim point of ACIS-S3. The count rates from this chip are higher than those of the front-illuminated chips, and local background can be measured from the large source-free area on the chip. There are several cases where significant interactions with bright cluster or group gas are likely and the radio sources are large (NGC 7385, 3C 442A, DA 240, 3C 35, 3C 326, 3C 236). However, multiple ACIS-I pointings would be required to cover the entire radio structures in three of these cases, and any outer X-ray emission is likely to be weak. In the other three cases we believe that the outer radio emission will correspond to little X-ray structure. Several low-redshift objects with similarly large angular sizes which have already been observed by *Chandra* show no significant features outside their central regions in similar-length observations.

ACIS-S count rates for the targets are given in Table 1. These count rates were computed using the AO-6 WWW-based version of `PIMMS`, with an intrinsic power-law spectrum with $\Gamma = 2.4$ and Galactic $N_{\rm H}$, and were based on *Einstein* or ROSAT count rates where possible. In a few cases the correlation between the radio and X-ray core flux densities had to be used (3C 35, 3C 76.1, 3C 192, PKS 1227+119, and 3C 285). For two cases the predicted flux densities exceeded the ROSAT All-Sky Survey limit, and so were reduced. Although some of the count rates are high and suggest pileup (3C 442A, 3C 310), in these cases almost all the counts come from group or cluster gas (Hardcastle & Worrall 1999). In no case will the pileup exceed 5% even in the unlikely event that all the compact (to ROSAT or *Einstein*) X-ray emission is concentrated at the core of the AGN.

We wish to take advantage of background event cleaning, and so request the use of VFAINT mode. To avoid telemetry overflow, we read out only four ACIS chips (ACIS-I2 and I3 with ACIS-S2 and S3), and reduce the energy range to $0.1 - 13.0$ keV. Counts between 10 and 13 keV will be used for flare monitoring. Finally, we provide roll angle preferences so that the faint readout streak from the core does not lie along the jet axis in any source. This will make detections of the jets more reliable, although the readout streaks will be faint in all cases, and so we do not constrain the roll angle more severely. The roll preferences do not conflict with AO-6 visibility for the sources.

3. Technical Feasibility for the HST Observations

Most 3CRR radio galaxies at low redshift have been imaged with WFPC-2 for 600 s or longer using the F555W and F702W filters. Many have been imaged in the UV with STIS. Important conclusions about the optical cores and the distribution of central gas have been reached based on these data, and optical fluxes for components of the jets have been a critical element in establishing the underlying electron energy distribution (e.g., Hardcastle et al. 2001). However the coverage is incomplete, and similar HST images are required if the full range of AGN structures is to be

Figure 3. The inner part of 3C 321 in the radio (1.5 GHz, contours) and X-ray (50 ks, ACIS-S, $0.5 - 7.0$ keV, greyscale). The core and inner jet of this FR II radio galaxy are well detected. HST data suggest that the jet bend and X-ray brightening are associated with an interaction with an adjacent galaxy. Bright X-ray emission is also detected from the radio hot spots further out on the ACIS-S3 chip (Hardcastle et al. 2004). A 40 ks ACIS-S exposure would be sufficient for this galaxy.

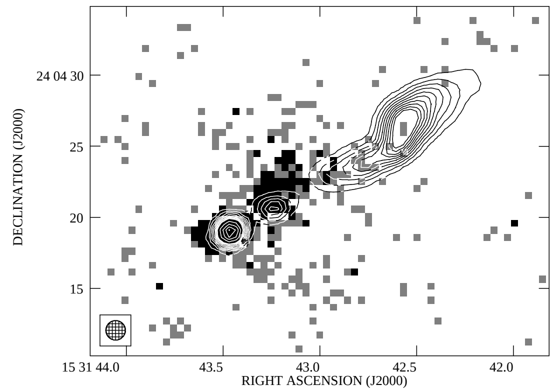

studied across all powers. We therefore request ACS/HRC exposures with F220W, and ACS/WFC exposures with F555W and F814W, for the eight galaxies 3C 386, NGC 7385, 3C 76.1, DA 240, 3C 310, 4C 73.08, 3C 452, and 1227+119. We will use a single orbit per object, and spend half ($\sim$ 1200 s, after overheads) on the F220W image and $\sim$ 600 s each on the F555W and F814W images (all with CR-SPLIT, and dither to avoid "Fastie finger" problems). In four cases one of these filters has already been observed, and we will extend the F220W exposure. The 26×29 arcsec HRC field at the core of each AGN is large enough to reveal any inner jet emission, central dust, and UV from the core, and the larger WFC field will cover the core and outer jets, and sometimes the hot spots. In standard backgrounds the images will detect at signal/noise > 10 any features brighter than 9.2×10^{-18}, 6.7×10^{-19}, and 3.0×10^{-19} erg cm^{-2} s^{-1} Å^{-1} in the F220W, F555W, and F814W filters. This improves on the existing Snapshot Survey data, though with the substitution of F814W for F702W, which is unavailable on ACS.

4. Analysis and Publication Strategy

Interest in the X-ray properties of 3CRR sources already spans many international groups of workers, and on average two data papers have already appeared in major refereed journals per observed sample object, even after excluding the famous galaxies 3C 231 (M 82), 3C 274 (M 87), and 3C 84 (NGC 1275). The data have prompted further papers on their theoretical interpretation. We expect the number of publications per 3CRR source to increase over the next few years as the *Chandra* archive is used to answer statistical questions.

Much of the multiwavelength data required to probe the physics of the sources is also public. We particularly note the excellent VLA coverage of the low-z 3CRR sources, and that the on-line VLA archive now makes these data highly accessible. *Spitzer* is observing many of the sources in GTO time, and we have submitted a GO proposal to complete the sample.

References

Brunetti, G.. et al. 2003. MNRAS 354, L40.
Chiaberge, M. et al. 2002. ApJ 571, 247.
de Koff, S. et al. 2000. ApJS 129, 33.
di Matteo, T. et al. 2003. ApJ 582, 133.
Fabbiano, G. et al. 1984. ApJ 277, 115.
Fabian, A.C. et al. 2000. MNRAS 318, L65.
Fabian, A.C. et al. 2003. MNRAS 344, L48.
Finoguenov, A., Jones, C. 2001. ApJ 547, L107.
Hardcastle, M.J., Worrall, D.M. 1999. MNRAS 309, 969.
Hardcastle, M.J., Worrall, D.M. 2000. MNRAS 314, 359.
Hardcastle, M.J. et al. 2001. MNRAS 326, 1499.
Hardcastle, M.J. et al. 2002a. MNRAS 334, 182.
Hardcastle, M.J. et al. 2002b. ApJ 581, 948.
Hardcastle, M.J. et al. 2004. In preparation.
Harris, D.A., Leighly, K.M., Leahy, J.P. 1998. ApJ 499, L149.

Table 1. The $z < 0.1$ 3CRR sample: sources to be observed with *Chandra* in **bold**

Name	z	N_H 10^{20} cm^{-2}	FR class	Line class	Environment	ACIS-S3 ct ks^{-1}	Archive ks
3C 231	0.0009	4.37	$*$	LE	g		20+
3C 272.1	0.0031	2.78	I	LE	cl		30
3C 274	0.0043	2.51	I	NL	cl		105+
3C 31	0.0167	5.53	I	LE	cl		50
3C 449	0.0171	11.05	I	LE	g		30
3C 84	0.0172	13.83	I	NL	cl		170+
3C 386	**0.0177**	**18.51**	**I**	**LE**	**g**	**19**	
3C 264	0.0208	2.20	I	LE	cl		40
3C 66B	0.0215	7.49	I	LE	cl		50
3C 296	0.0237	1.85	I	LE	i		50
NGC 6251	0.0240	5.52	I/II	LE	cl		50+
NGC 7385	**0.0243**	**4.85**	**I**	**LE**	**cl**	**74**	
3C 83.1B	0.0255	13.86	I	LE	cl		95
3C 442A	**0.0263**	**5.08**	**I/II**	**LE**	**cl**	**115**	
3C 465	0.0293	4.91	I/II	LE	cl		50
NGC 6109	0.0296	1.47	I	LE	cl		20
3C 338	0.0298	0.88	I/II	NL	cl		20+
3C 98	**0.0306**	**11.70**	**II**	**NL**	**i**	**8**	
3C 76.1	**0.0324**	**10.10**	**I/II**	**LE**	**i**	**29**	
DA 240	**0.0356**	**4.62**	**II**	**LE**	**i**	**20**	
3C 305	**0.0417**	**1.68**	**I/II**	**NL**	**g**	**9**	
3C 293	**0.0452**	**1.29**	**I**	**LE**	**i**	**3**	
3C 310	**0.0540**	**3.42**	**I/II**	**LE**	**g**	**121**	
3C 390.3	0.0569	4.17	II	BL	g		35
3C 382	0.0578	7.28	II	BL	g		120 †
4C 73.08	**0.0581**	**2.45**	**II**	**NL**	**g**	**10**	
3C 33	**0.0595**	**3.92**	**II**	**NL**	**cl**	**13**	
3C 192	**0.0598**	**4.31**	**II**	**NL**	**g**	**4**	
3C 35	**0.0677**	**13.12**	**II**	**LE**	**cl**	**21**	
3C 285	**0.0794**	**1.37**	**II**	**NL**	**cl**	**26**	
3C 452	0.0811	11.30	II	NL	i		80
1227+119	**0.0837**	**2.43**	**I**	**LE**	**g**	**31**	
3C 326	**0.0895**	**3.87**	**II**	**NL**	**i**	**2**	
3C 388	0.0908	5.81	II	LE	cl		40 I
3C 321	0.0960	4.10	II	NL	i		50
3C 236	**0.0989**	**1.26**	**II**	**LE**	**i**	**3**	

FR class: $*$ = starburst galaxy. Line class: BL = broad lines; NL = strong narrow lines; LE = low excitation lines ([OIII]/H$\alpha < 0.2$, [OIII] eq. width < 3Å). Environment: cl = cluster; g=group; i = isolated. Archive ACIS-S: + = multiple observations; † = HETGS observation with good zero-order image; I = ACIS-I observation.

Georganopoulos, M., Kazanas, D., 2002. ApJ 589, L5.
Laing, R.A., Bridle, A. 2002. MNRAS 336, 1161.
Laing, R.A., Riley, J.M., Longair, M.S. 1983. MNRAS 204, 151.
Martel, A. et al. 2000. ApJS, 130, 267.
Owen, F.N., Ledlow, M. 1994. *The Physics of Active Galaxies*, ASP Conf. Ser. 54, 319.
Perlman, E., Wilson, A.S., 2004. In preparation.
Tansley, D. et al. 2004. MNRAS submitted.
Wilson, A.S., Yang, Y. 2002. ApJ 568, 133.
Worrall, D.M., Birkinshaw, M., 1994. ApJ 427, 134.

Previous *Chandra* **Programs.** As PI: 01700490, 01700598, 02700703, 03700795, 04700285, 04700407

Chandra **Publications**

2000 The Chandra X-ray Observatory Resolves the X-ray Morphology and Spectra of a Jet in PKS 0637-752 (Chartas, G., Worrall, D.M., **Birkinshaw, M.**, 14 authors, ApJ, 542, 655–666.

2000 Chandra Discovery of a 100 kpc X-ray jet in PKS 0637-752 (Schwartz, D.A., 4 authors, **Birkinshaw, M.**, 14 authors) ApJ, 540, L69–L72.

2001 A Chandra detection of the radio hotspot of 3C 123 (Hardcastle, M.J., **Birkinshaw, M.** & Worrall, D.M.) MNRAS, 323, L17–L22.

2001 Chandra finds X-ray jets are common in low-power radio galaxies (Worrall, D.M., **Birkinshaw, M.** & Hardcastle, M.J.) MNRAS, 326, L7–L12.

2001 Chandra measurements of the X-ray core and cluster of 3C 220.1 (Worrall, D.M., **Birkinshaw, M.**, Hardcastle, M.J. & Lawrence, C.R.) MNRAS, 326, 1127–1133.

2001 Chandra observations of the X-ray jet in 3C 66B (Hardcastle, M.J., **Birkinshaw, M.** & Worrall, D.M.) MNRAS, 326, 1499–1507.

2001 New insights on Radio-Galaxy X-ray emission components from Chandra (Worrall, D.M., **Birkinshaw, M.** & Hardcastle, M.J.) ASP Conference Series, vol 234, 485–492

2001 Chandra Observations of the PKS 0637-752 X-ray Jet (Schwartz, D.A., 12 authors, **Birkinshaw, M.**, 7 authors) ASP Conference Series, vol 234, 493–499

2002 A Chandra observation of the X-ray environment and jet of 3C 31 (Hardcastle, M.J., Worrall, D.M., **Birkinshaw, M.**, Laing, R.A. & Bridle, A.H.) MNRAS, 334, 182–192.

2002 New radio-galaxy X-ray results from Chandra (Worrall, D.M., **Birkinshaw, M.** & Hardcastle, M.J.) ASP Conference Series, vol 250, 224–229

2002 Equipartition in the hotspots of 3C 123 (Hardcastle, M.J., **Birkinshaw, M.** & Worrall, D.M.) ASP Conference Series, vol 250, 234–237

2002 The X-ray jet and halo of PKS 0521-365 (**Birkinshaw, M.**, Worrall, D.M., & Hardcastle, M.J.) MNRAS, 335, 142–150.

2002 Magnetic Field Strengths in the hotspots & lobes of 3 powerful FRII radio sources (Hardcastle, M.J., **Birkinshaw, M.**, Cameron, R.A., Harris, D.E., Looney, L.W. & Worrall, D.M.) ApJ, 581, 948–973

2003 The X-ray Emission of Low-power Radio Galaxies (Worrall, D.M., **Birkinshaw, M.**, & Hardcastle, M.J.) ASP Conference Series, vol 290, 363–365

2003 Results from a Complete *Chandra* Survey of Radio Jets (Schwartz, D.A., Marshall, H.L., Miller, B.P., Worrall, D.M., **Birkinshaw, M.**, 5 authors) ASP Conference Series, vol 290, 359–360

2003 *Chandra* Observations of X-ray Jet Structure on kpc to Mpc scales (Schwartz, D.A., Marshall, H.L., Miller, B.P., Worrall, D.M., **Birkinshaw, M.**, 5 authors) New Astronomy Review, 47, 461–465

2003 The X-ray Jet and Central Structure of the Active Galaxy NGC 315 (Worrall, D.M., **Birkinshaw, M.**, & Hardcastle, M.J.) MNRAS, 343, L73–L78

2004 Equipartition and Magnetic Fields in Radio Sources (**Birkinshaw, M.**, Worrall, D.M. & Hardcastle, M.J.) ESA SP-488, in press

2004 The kpc-scale X-ray jets of radio-loud AGN (Worrall, D.M., **Birkinshaw, M.** & Hardcastle, M.J.) ESA SP-488, in press

2004 The hotspots of Cygnus A (Wright, M.C.H. & **Birkinshaw, M.**) ApJ, in press

2004 Chandra Observations of NGC 4261 (3C 270): Revealing the hidden AGN in a type-2 liner (Zezas, A., **Birkinshaw, M.**, Worrall, D.M., Peters, A., & Fabbiano, G.) ApJ, submitted